Efficient and Targeted Transduction of Nonhuman Primate Liver With Systemically Delivered Optimized AAV3B Vectors

Shaoyong Li[1,2], Chen Ling[3,4], Li Zhong[1,5,6], Mengxin Li[1,2,6], Qin Su[5], Ran He[5], Qiushi Tang[1,6], Dale L Greiner[7], Leonard D Shultz[8], Michael A Brehm[7], Terence R Flotte[1,6], Christian Mueller[1,6], Arun Srivastava[3,4] and Guangping Gao[1,2,5]

[1]Horae Gene Therapy Center, University of Massachusetts Medical School, Worcester, Massachusetts, USA; [2]Department of Microbiology and Physiology Systems, University of Massachusetts Medical School, Worcester, Massachusetts, USA; [3]Powell Gene Therapy Center, University of Florida, Gainesville, Florida, USA; [4]Division of Cellular and Molecular Therapy, Department of Pediatrics, University of Florida, Gainesville, Florida, USA; [5]Viral Vector Core, University of Massachusetts Medical School, Worcester, Massachusetts, USA; [6]Department of Pediatrics, University of Massachusetts Medical School, Worcester, Massachusetts, USA; [7]Program in Molecular Medicine, University of Massachusetts Medical School, Worcester, Massachusetts, USA; [8]The Jackson Laboratory Bar Harbor, Bar Harbor, Maine, USA

Recombinant adeno-associated virus serotype 3B (rAAV3B) can transduce cultured human liver cancer cells and primary human hepatocytes efficiently. Serine (S)- and threonine (T)-directed capsid modifications further augment its transduction efficiency. Systemically delivered capsid-optimized rAAV3B vectors can specifically target cancer cells in a human liver cancer xenograft model, suggesting their potential use for human liver-directed gene therapy. Here, we compared transduction efficiencies of AAV3B and AAV8 vectors in cultured primary human hepatocytes and cancer cells as well as in human and mouse hepatocytes in a human liver xenograft NSG-PiZ mouse model. We also examined the safety and transduction efficacy of wild-type (WT) and capsid-optimized rAAV3B in the livers of nonhuman primates (NHPs). Intravenously delivered S663V+T492V (ST)-modified self-complementary (sc) AAV3B-*EGFP* vectors led to liver-targeted robust enhanced green fluorescence protein (EGFP) expression in NHPs without apparent hepatotoxicity. Intravenous injections of both WT and ST-modified rAAV3B.ST-*rhCG* vectors also generated stable super-physiological levels of rhesus chorionic gonadotropin (rhCG) in NHPs. The vector genome predominantly targeted the liver. Clinical chemistry and histopathology examinations showed no apparent vector-related toxicity. Our studies should be important and informative for clinical development of optimized AAV3B vectors for human liver-directed gene therapy.

Received 19 July 2015; accepted 14 September 2015; advance online publication 27 October 2015. doi:10.1038/mt.2015.174

INTRODUCTION

Adeno-associated virus (AAV) is a small single-stranded DNA-containing nonpathogenic human parvovirus, which has gained attention as an efficient and safe gene transfer vehicle. Systemic delivery of some AAV serotypes has shown a liver tropism, which makes them ideal choices for liver-directed gene therapy.[1] Recombinant AAV (rAAV), mainly AAV2, has been used in a number of liver-directed gene therapy clinical trials, including treatment of hemophilia.[2,3] Recently, a systemically delivered self-complementary (sc) AAV serotype 8 vector led to clinical efficacy in a hemophilia B gene therapy trial.[3] However, the presence of neutralizing antibodies,[4,5] and $CD8^+$ T-cell responses[2,3,6] against those AAV capsids in humans may limit the possible application of rAAVs for liver gene therapy. To overcome this dose- and serotype of AAV capsid-dependent adaptive immune responses in humans, the development of alternative serotypes of highly human liver-tropic AAV vector is critical to achieving effective, sustained, and safe liver-directed gene therapy.

In our recent studies,[7,8] we have documented that rAAV3B vectors transduce cultured human liver cancer cell lines and primary human hepatocytes efficiently because AAV3B uses human hepatocyte growth factor receptor (huHGFR) as a cellular coreceptor. We have also reported that the next generation of rAAV2 vectors containing mutations in the surface-exposed tyrosine (Y),[9,10] serine (S),[11] and/or threonine (T)[12] residues transduce murine hepatocytes exceedingly well at lower doses. Additionally, we have generated tyrosine-mutant rAAV3B serotype vectors, and identified an optimized vector that efficiently transduces human liver tumors in a murine xenograft model *in vivo*.[13] In an attempt to further enhance the transduction efficiency of rAAV3B vector, we evaluated AAV3B vectors containing various combinations of mutations in the surface-exposed Y, S, and T residues

The first three authors contributed equally to this work.

Correspondence: *Guangping Gao, Horae Gene Therapy Center, University of Massachusetts Medical School, Worcester, Massachusetts, USA. E-mail: guangping.gao@umassmed.edu or Arun Srivastava, Powell Gene Therapy Center, University of Florida, Gainesville, Florida, USA. E-mail: aruns@peds.ufl.edu Correspondence regarding the liver xenograft model should be addressed to Christian Mueller, Horae Gene Therapy Center, University of Massachusetts Medical School, Worcester, Massachusetts, USA. E-mail: Chris.Mueller@umassmed.edu)*

and identified an S633V+T492V mutant (AAV3B.ST) with the best capacity to transduce human liver tumor cells and primary human hepatocytes *in vitro*.[14,15] Moreover, the use of the rAAV3B-ST vectors not only led to targeted delivery and suppression of human liver tumorigenesis in a murine xenograft model, in our preliminary studies, it also resulted in efficient transduction of humanized murine livers *in vivo*.[14] In a more recent attempt to evolve novel AAV capsids that can target human hepatocytes for gene delivery, Lisowski *et al.*[16] isolated a novel capsid variant of AAV3B, designated LK03, through several rounds of selection of a shuffled capsid library in a human liver xenograft mouse model.[16] LK03, a close relative of AAV3B with eight amino acids that are different from AAV3B, showed strong tropism in human hepatocytes *in vivo* in humanized mouse liver, suggesting that AAV3B-based vectors could be a safe and effective alternative to AAV8 vectors for liver-targeted gene therapy in humans. Importantly, the presumably low levels of pre-existing antibodies to AAV3B in the human population could also make rAAV3B highly attractive for its clinical applications.[17–20]

Although murine xenograft and humanized mouse models provide a useful model system to test the efficacy of optimized rAAV3B vectors in human hepatocyte transduction, the safety of these vectors cannot be evaluated in such models since rAAV3B vectors do not transduce any tissues or organs in mice.[8,21] On the other hand, a translational study of those vectors in nonhuman primates (NHPs) may at least provide some corroborating evidence with reference to these aspects of the vector biology because of the closeness of phylogenetic and physiology between NHPs and humans.[22–25] To evaluate the safety and efficacy of the systemically delivered optimized rAAV3B vectors prior to their potential use in human gene therapy, we pursued the current studies to evaluate transduction efficiency of AAV3B in human hepatocytes *in vitro* and *in vivo*; we also evaluated the transduction efficacy as well as biodistribution and safety profiles of optimized rAAV3B in NHPs after systemic administration. To this end, we first compared transduction efficiencies of AAV3B and AAV8 vectors in primary human hepatocytes and human cancer cell lines *in vitro* as well as in human and mouse hepatocytes *in vivo* using a human liver xenograft mouse model. We next investigated sero-epidemiology of AAV3B in a rhesus monkey colony and found that the pre-existing neutralized antibodies (NAb) against AAV3B are relatively lower (48% of animals with detectable NAb) as compared with AAV8 (≥75% of animals positive for AAV8 NAb) in rhesus macaques. We first used EGFP reporter gene vector to assess liver-tropism of scAAV3B.ST in NHPs; the results indicated that optimized AAV3B.ST vector produced robust and specific EGFP expression in the liver, but not in any other tissues analyzed, with no apparent hepatotoxicity. To quantitatively assess transduction efficiency of WT scAAV3B and the scAAV3B.ST vectors in NHP liver, we intravenously dosed rhesus macaques (n = 3 per vector group) with both WT- and ST-modified scAAV3B vectors expressing a secreted reporter gene, rhesus chorionic gonadotropin (rhCG). The results revealed that both vectors led to efficient and sustained rhCG expression up to 3 months (the duration of the study), but ST-modified scAAV3B led to fivefold (at early stage) and twofold (at late stage) enhanced rhCG expression compared with its WT counterpart. This was confirmed with quantitative reverse transcription polymerase chain reaction (qRT-PCR) analysis of liver rhCG mRNA levels at the day 91 end-point, showing again a twofold increased rhCG transcripts in hepatocytes transduced by the ST-modified AAV3B vectors. The biodistribution analysis of the persisting vector genomes displayed a liver predominant pattern. Clinical chemistry and histopathology studies also showed no apparent vector-related toxicity for both vectors in the study animals.

RESULTS

Transduction efficiency of scAAV3B vectors in primary human hepatocytes *in vitro* and *in vivo*

We first compared the *in vitro* transduction efficiency of self-complementary (sc) AAV2, scAAV3B, and scAAV8 vectors in three different human cell types, HeLa (cervical cancer cell), Huh7 (liver cancer cell), and primary human hepatocytes (**Figure 1**). All vectors expressed the Gaussia Luciferase (GLuc) reporter gene under the control of the cytomegalovirus (CMV) enhancer/chicken β-actin hybrid promoter (CB). Consistent with previous reports,[26,27] scAAV8 vector inefficiently transduces any cell types *in vitro*. In comparison to scAAV2, which efficiently transduced HeLa cells, rAAV3B preferentially transduced both human liver cancer cells (threefold versus scAAV2) and normal hepatocytes (10-fold versus scAAV2), further corroborating the human liver cell-restricted specificity of AAV3B vectors.

To compare AAV3B and AAV8 vectors for transduction efficiencies in human and mouse hepatocytes *in vivo*, we utilized a newly created NSG-PiZ mouse model (see methods). NSG-PiZ mouse livers were repopulated with primary human hepatocytes. The human liver xenograft was monitored prospectively by sampling mouse sera and measuring human albumin levels. As shown in **Figure 2a**, the chimeric livers resulted in stable serum levels of human albumin between 0.4 and 2.8 mg/ml. Engrafted and nonengrafted NSG-PiZ mice were intravenously injected with rAAV3B or rAAV8-CB-FFLuc vectors at a dose of 1×10^{11} viral genomes (vgs)/mouse. Whole body Firefly Luciferase

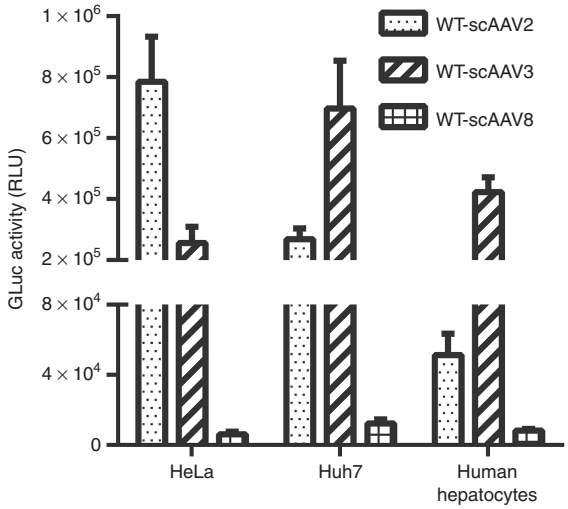

Figure 1 Transduction efficiency of scAAV vectors *in vitro*. Cultured HeLa, Huh7, and primary human hepatocytes were transduced with wild-type (WT) scAAV2, scAAV3B, or scAAV8-CB-*GLuc* vectors. The Gluc expression in the medium was determined 72 hours postinfection.

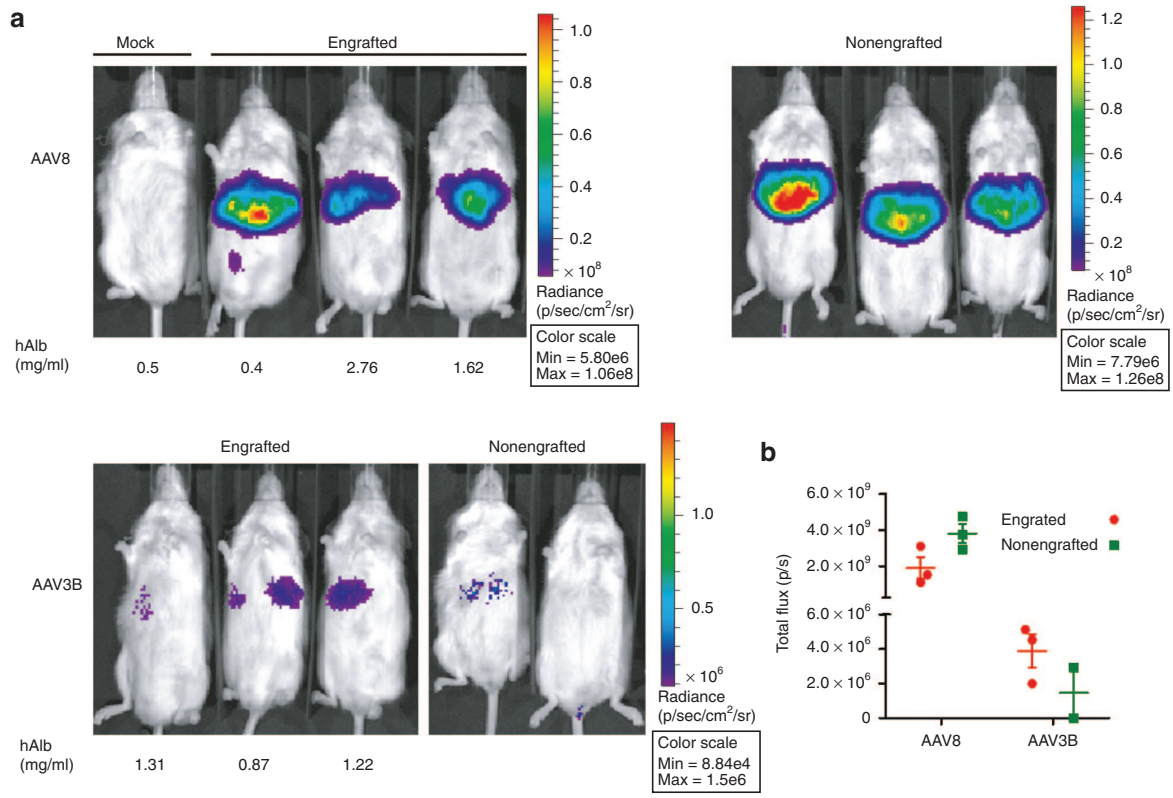

Figure 2 ***In vivo*** **detection of Firefly Luciferase (FFLuc) transduction of naive and humanized mouse liver by intravenously delivered AAV8 and AAV3B vectors.** Adult male NSG-PiZ mice were repopulated with primary human hepatocytes. Four weeks later, mice were intravenously injected with either scAAV3B or scAAV8-CB-*FFLuc* vectors at a dose of 1×10^{11} GCs/mouse. Nonengrafted NSG-PiZ mice were used as appropriate controls. (**a**) Mice whole body *in vivo* imaging was taken at 2-week after vector infusion. (**b**) Quantitative comparison of *in vivo* FFLuc activities in mouse livers that were engrafted and nonengrafted with primary human hepatocytes and treated with different serotypes of AAV vectors.

(FFLuc)-based bioluminescence images taken at 2-week post-vector infusion are shown in **Figure 2a**. *In vivo* FFLuc bioluminescence was quantified for the abdominal region of interest as presented for each serotype (**Figure 2b**). The data demonstrates that rAAV8-treated animals had ~3 logs higher FFLuc bioluminescence as compared with rAAV3B-injected mice, regardless of engraftment status of the mice (**Figure 2a**,**b**). However, human hepatocyte engraftment did seem to reduce FFLuc luminescence by half in the rAAV8 group while the luminescence was doubled in the rAAV3B mice that were engrafted with human hepatocytes (**Figure 2a**,**b**). To differentiate the contributions of human and mouse hepatocytes to luciferase activity in the human liver xenografts, we performed immunofluorescence analysis of liver tissue sections. Engrafted human hepatocytes were identified by staining with a human albumin (huAlb) specific antibody (red), while an FFLuc specific antibody (green) was used for detecting rAAV transduction. To determine the ability of each serotype to transduce human hepatocytes, we quantified double-positive hepatocytes (huAlb+FFLuc+) with the merged (orange) fluorescence by using the ImarisColoc program. The double-positive hepatocytes (huAlb+FFLuc+) in the engrafted livers were 50.3 ± 7% for rAAV8 and 27.7 ± 3.7% for rAAV3B group. In addition, a quantitative analysis for the hepatocytes that were positive only for FFLuc staining revealed that 47.1 ± 4.7% of mouse hepatocytes were transduced by rAAV8, whereas only 2.51 ± 2.3% of the cells were positive for rAAV3B transduction (**Figure 3**). Our data indicate that *in vivo* rAAV8 transduces mouse hepatocytes much more (~20-fold) efficiently than rAAV3B, which is consistent with the published data by Lisowski *et al.*[16] However, our data also suggests that both rAAV8 and rAAV3B can transduce engrafted human hepatocytes at similar efficiencies. Despite this discrepancy from what was reported by Lisowski *et al.*, these results nonetheless suggest that scAAV3B vectors selectively transduce human hepatocytes *in vivo*.

Assessment of pre-existing and postinjection NAb and IgGs against AAV3B in rhesus macaque population

Considering the relatively low prevalence of pre-existing anti-AAV3B capsid antibodies in the human population,[17–20] AAV3B could be an ideal vector for liver-target gene therapy in humans. To test the prevalence of pre-existing antibodies against AAV3B in NHPs and to prevent any NAb-related transduction suppression, the animals were screened and selected prior to initiating the *in vivo* studies based on the assumption that AAV3B and AAV3B.ST behave serologically similarly.[19] Fifty-two percent of rhesus macaques displayed no detectable NAb at a detection limit of NAb = 1:5, which was the selection criterion for the animals enrolled in the study (**Supplementary Tables S1 and S2**). To monitor the humoral immune response against the AAV capsid after i.v. administration of viral vectors, the animals were tested for NAb at different time points postinjection of

both WT AAV3B and AAV3B.ST vectors (**Table 1**). From −14 days to the injection day, the animals were all Nab-negative for AAV3B. As previously reported,[28–30] at the day 7 postinjection, the titers of NAb were significantly increased in all animals as expected. After 3 months, the NAb titers were either stable or declined slightly. The humoral response against the capsids of WT AAV3B and AAV3B.ST vectors in the study macaques was further characterized by measuring capsid specific total IgG and its subtypes IgG1, IgG2, and IgG4 in the serum samples. As what was observed for the NAb titers, the IgG analysis also revealed a trend of remarkable increases in capsid specific total IgG and IgG2 subtypes but not IgG1 and IgG4, starting at as early as day 7 postvector infusions (**Supplementary Table S3**).

Noticeably, the monkey #133–2012 generated the highest NAb titer (1/1,280) of all animals at day 7 postinjection. Interestingly, this monkey also displayed a declined rhCG expression as well as moderately elevated alanine aminotransferase (ALT) and aspartate aminotransferase (AST) levels at day 7 postvector infusion (**Supplementary Table S4**). Thus, the immune response against AAV3B vectors following vector delivery seemed to be highly variable among individual animals, which might have contributed to the variable levels of transgene expression observed in different animals.

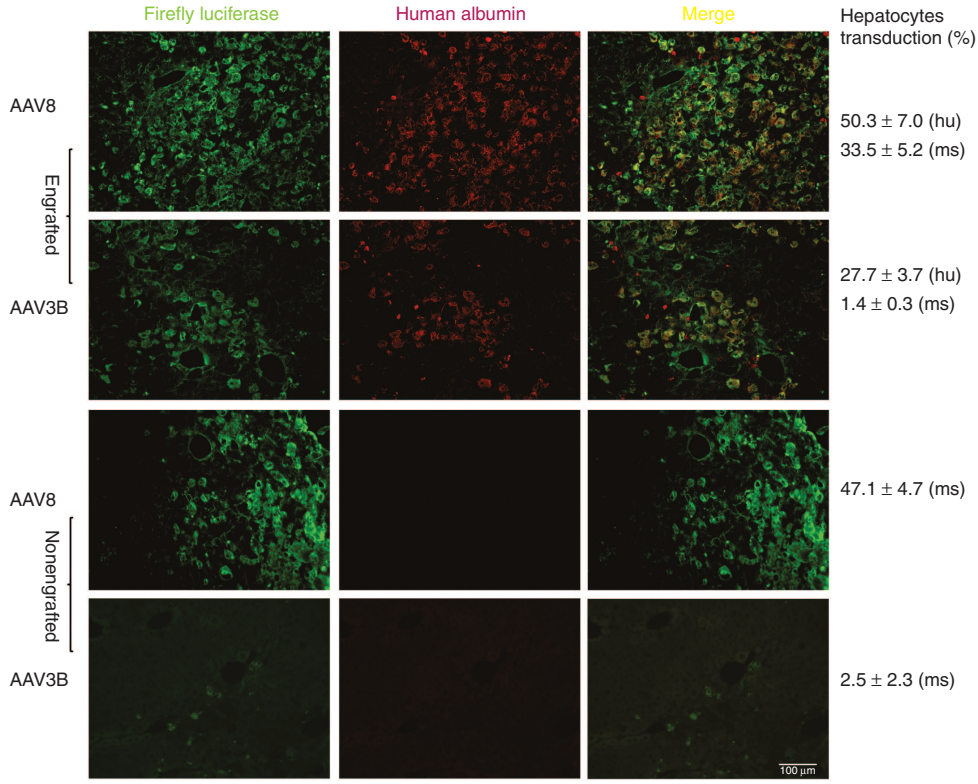

Figure 3 Comparison of FFLuc transduction efficiencies in human and mouse hepatocytes in a human liver xenograft NSG-PiZ mouse model by AAV3B and AAV8 vectors using immunofluorescent staining. Four weeks after vector administration, the livers were harvested, sectioned, stained for firefly luciferase (green) and human albumin (red), and analyzed using Leica DM-5500 microscope. The merged images (orange) show human hepatocytes transduced by rAAV serotype vectors. Representative images of stained liver sections were presented. For quantitative comparison, the percentages of FFLuc transduced human and mouse hepatocytes were estimated by ImarisColoc (Imaris, Bitplane). Scale bar = 100 µm.

Table 1 The titer of the neutralized antibodies against AAV3B in rhesus macaques before and after vector injections

		Time (days)									
Animal ID	**Treatment**	**−14**	**−7**	**0**	**7**	**21**	**35**	**49**	**63**	**77**	**91**
22–2012	WT scAAV3B-*rhCG*	<1/5	<1/5	<1/5	1/160–1/320	>1/20	1/80–1/160	>1/20	>1/20	>1/20	1/80–1/160
106–2012	WT scAAV3B-*rhCG*	<1/5	<1/5	<1/5	1/80–1/160	>1/20	1/40–1/80	>1/20	1/10–1/20	1/10–1/20	1/10–1/20
110–2012	WT scAAV3B-*rhCG*	<1/5	<1/5	<1/5	1/80–1/160	>1/20	1/40–1/80	>1/20	>1/20	>1/20	1/160–1/320
133–2012	scAAV3B.ST-*rhCG*	<1/5	<1/5	<1/5	1/640–1/1280	>1/20	1/320–1/640	>1/20	>1/20	>1/20	1/160–1/320
136–2012	scAAV3B.ST-*rhCG*	<1/5	<1/5	<1/5	1/40–1/80	>1/20	1/40–1/80	>1/20	>1/20	>1/20	1/20–1/40
176–2012	scAAV3B.ST-*rhCG*	<1/5	<1/5	<1/5	1/80–1/160	>1/20	1/160–1/320	>1/20	>1/20	>1/20	1/160–1/320

Liver-targeted robust transgene expression in rhesus macaques after systemic administration of optimized scAAV3B.ST-*EGFP* vector

As the optimized scAAV3B.ST transduces cultured human primary hepatocytes and humanized mouse liver efficiently, we hypothesized that scAAV3B.ST might also be highly tropic for NHP liver. To test this hypothesis, we infused adult male rhesus macaques (n = 3) with scAAV3B.ST-*EGFP* vector via cephalic vein at the dosage of 1×10^{13} GC/kg and collected tissues at the day 7 postinjection for analysis. As shown in **Figure 4a**, robust EGFP expression was detected in all four liver lobes of all study animals. Quantitative analyses confirmed that, in average, approximately 36% of total areas in each visual field of liver sections from different lobes of different animals were EGFP positive (**Figure 4b**). However, little evidence of EGFP gene expression was observed in any other 11 tissues analyzed (*i.e.*, heart, skeletal muscle, pancreas, testis, lung, kidney, spleen, pancreas, GI tract (jejunum and colon), and brain); data from four of which is presented in **Supplementary Figure S1**. These data clearly reveal liver-restricted transgene expression in rhesus macaques following systemic delivery of scAAV3B.ST vectors.

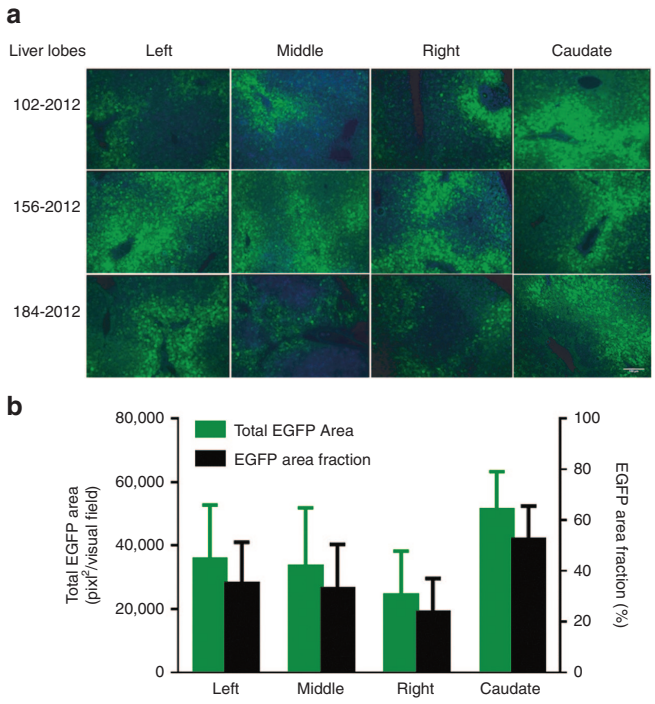

Figure 4 Efficient enhanced green fluorescence protein (EGFP) liver transduction by scAAV3B.ST-*EGFP* vector in rhesus macaques. (**a**) Rhesus monkeys were i.v. injected with scAAV3B.ST-*EGFP* vectors (1×10^{13} GC/kg) via cephalic vein infusion. The liver sections were fixed and transgene expression was detected by fluorescence microscopy at day 7 postinjection. Original magnification ×100, scale bar = 100 µm. (**b**) Quantitative analyses of scAAV3B.ST-*EGFP* transduction efficiency. Images from one visual field of each liver lobe were analyzed quantitatively using ImageJ analysis software. Transgene expression was assessed as total area of green fluorescence (pixel2) (left y-axis) and area fraction per visual field (right y-axis) (mean ± SEM).

Quantitative assessment of transduction efficiency and biodistribution of WT and optimized ST-modified scAAV3B vectors in rhesus macaques

To quantitatively assess the transduction efficiency of systemically delivered WT AAV3B and optimized AAV3B.ST vectors, we generated the vectors expressing a secreted self-antigen, rhCG, as a quantitative reporter gene in rhesus macaques. Both WT and ST-modified AAV3B vectors displayed similar onset and kinetics of rhCG expression with peak levels around 10^4–10^5 rU/ml and gradual decline to 2×10^4 rU/ml in average by the end point (day 91). However, average rhCG expression from AAV3B.ST was fivefold higher at peak ($P < 0.01$) and twofold higher at day 91 ($P > 0.05$) as compared with WT AAV3B vector (**Figure 5a**). The rhCG mRNA expression level in the liver from AAV3B.ST was also twofold higher at day 91 as compared with WT AAV3B vector, although there was no statistical significance (**Figure 5b**). As would be expected for outbred animals, substantial animal-to-animal variations were observed in the three monkeys that received the AAV3B.ST vector; one animal (#133–2012) displayed the sharpest decline in transgene expression immediately after the 1-week time point, from 5.5×10^4 rU/ml at week 1 to 1.9×10^4 rU/ml at week 3, a 66% reduction for #133–2012 as compared with no decline in the second animal, and 40% reduction in the third animal in the same AAV3B.ST vector group. The rhCG levels of animal #133–2012 continued to decline to 7% of the peak level (week 1) by the end of the study (day 91), while the serum rhCG levels in the other two animals were 48 and 21% of the week 1 levels, respectively. Furthermore, at the time of necropsy, the liver rhCG mRNA in this monkey was also the lowest (**Figure 5b**) in the same group (0.36-fold compared with 4.9- and 1.2-fold, respectively, for the other two monkeys).

The AAV vector genome biodistribution profiles in all study animals were also assessed by quantitative polymerase chain reaction (qPCR). The vector genomes of both WT and AAV3B.ST vectors were predominantly enriched in the liver, up to 25 GC/cell for AAV3B.ST vector, as expected, followed by spleen, kidney, heart, adrenal gland, and pancreas (**Figure 6a**). Although not statistically significant ($P = 0.12$), it was noticeable that fewer vector genomes were detected in the hearts of the animals that received the AAV3B.ST vector (**Figure 6a**). We further analyzed six organs (liver, spleen, heart, kidney, adrenal gland, and skeletal muscle) with relative higher AAV genome copies for rhCG mRNA expression. Despite high vector genome copy number in the spleen, no transgene expression was detected, and the levels of rhCG mRNA also correlated well with vector genome abundance with highest levels in the liver in both WT- and AAV3B.ST vector-injected groups (**Figure 6b**).

Lack of apparent vector-related toxicity in rhesus macaques following systemic delivery of WT and AAV3B.ST vectors

To evaluate the safety of both WT AAV3B and rAAV3B.ST vectors, we monitored the animals for clinical abnormality, clinical chemistries and hematology throughout the 3 months duration of the study. Overall, there was no noticeable abnormality in any of clinical parameters observed in all nine study animals (**Supplementary Table S4**). The blood chemical parameters,

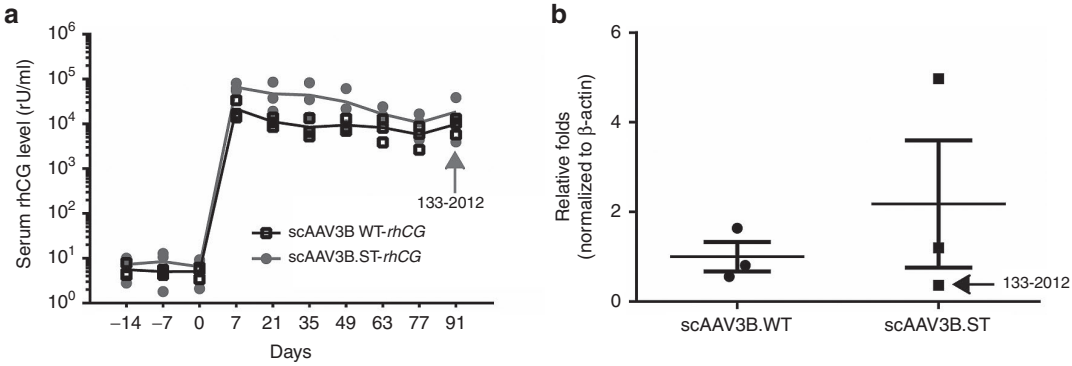

Figure 5 rhCG expression from wild-type (WT)- and ST-modified rAAV3B.*rhCG* vectors at different time points in rhesus macaques. (**a**) Monkey sera were collected at different time points after i.v. injection of rAAV3B WT-*rhCG* and rAAV3B.ST-*rhCG* (1×10^{13} GC/kg). The serum rhCG levels were detected by enzyme-linked immunosorbent assay. rhCG standard was generated by transfecting rhCG expression plasmids into Huh7.5 cells and collecting the supernatant. Undiluted supernatant was arbitrarily assigned a concentration of 6,400 rU/ml (where rU = relative units). (**b**) Relative liver rhCG mRNA expression of animal groups received rAAV3B WT-*rhCG* and rAAV3B.ST-*rhCG* at day 91 postinjection were detected by reverse transcription followed by Taqman qPCR. β-actin was used as internal control for qPCR. Student *t*-test was used for comparing the experimental results from the groups of rAAV3B WT-*rhCG* and rAAV3B.ST-*rhCG*, and the differences were determined to be statistically significant. $^{**}P < 0.01$; $^{*}P < 0.05$.

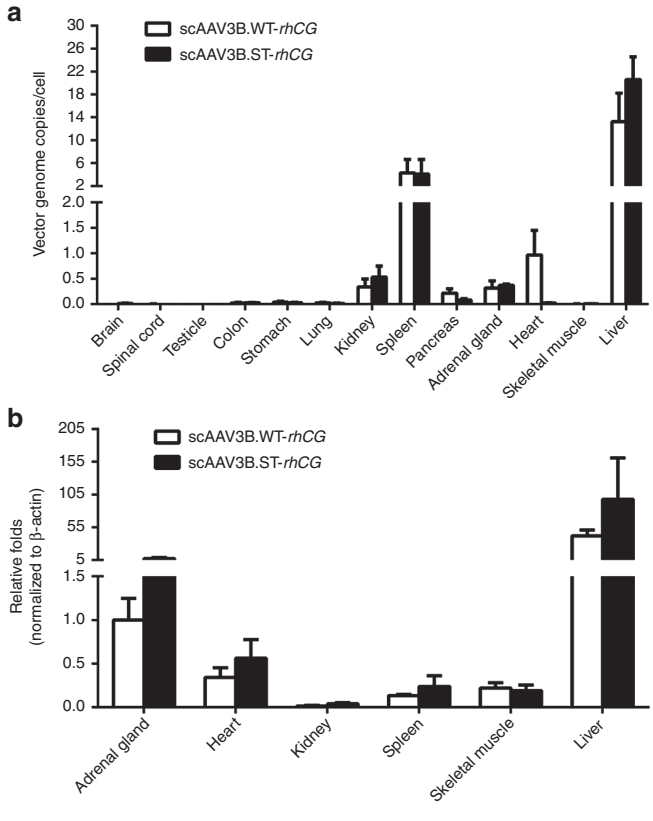

Figure 6 Biodistribution of vector genomes and rhCG mRNA expression in rhesus macaques after systemic administration of WT- and ST-modified rAAV3B.*rhCG*. Monkey tissues were collected at day 91 postinjection of rAAV3B WT-*rhCG* and rAAV3B.ST-*rhCG* (1×10^{13} GC/kg). (**a**) Tissue DNA was isolated as described in the Methods. qPCR was performed to measure the AAV genome copies per diploid cell. (**b**) Tissue mRNA was isolated from six selected organs as described in the Methods. RT-qPCR was performed to measure the rhCG mRNA expression level. $^{**}P < 0.01$; $^{*}P < 0.05$. No significant difference among all groups was observed.

including ALT (**Figure 7a**) and AST (**Figure 7b**), were in normal range during the study for both WT AAV3B and rAAV3B.ST vector-injected groups. However, it is noteworthy that at the day 7 postinjection of scAAV3B.ST-*rhCG* vector, both the ALT and AST levels in the monkey #133–2012 increased moderately, up to two- and threefold, respectively, as compared with the levels at day −7 (**Figure 7c,d**). Such a moderate transaminitis in this animal around day 7 most likely was the underlying cause for the observed decline in rhCG expression at later time points.

Histopathological analysis of tissues and organs of all animals necropsied at day 91 was performed as described under Materials and Methods. All treated monkeys were grossly and clinically normal. There were no signs of irritation at the injection site and no evidence of intercurrent bacterial or viral infections or malformations. Hematoxylin and Eosin stained liver and spleen tissue sections also showed no apparent abnormality (**Supplementary Figure S2a,b**). The same analysis performed in nine other organs, including brain, bone marrow, colon, heart, kidney, lung, lymph node, small bowel, and testes, provided no evidence of pathological lesions (data not shown).

DISCUSSION

Liver has long been considered among the ideal targets for the potential gene therapy of a wide variety of human diseases using recombinant AAV vectors ever since we and others first described the hepatotropic nature of AAV2 vectors, albeit for the murine liver.[31,32] Indeed, the first generation of AAV2 vectors were used in a phase 1 clinical trial for hemophilia B.[2] Unfortunately, however, despite highly encouraging preclinical studies performed using murine and canine models of hemophilia B,[33] the corresponding ssAAV2 vector dose failed to express therapeutic levels of the clotting factor IX (F.IX) in a patient, and although the use of a 10-fold higher vector dose did lead to clinical efficacy in a second patient, it was short-lived due to complications involving a $CD8^+$ cell-mediated cytotoxic T-cell response against AAV2 capsid proteins. A subsequent clinical trial with scAAV8 vectors[3] proved to be a significant step forward, but a similar immune response was also observed in the high-dose cohort of patients.[34] Although the choice of AAV8 vector was undoubtedly based on its superior performance over AAV2 vectors in transducing murine hepatocytes, it was not readily apparent whether AAV8 vectors would be ideal

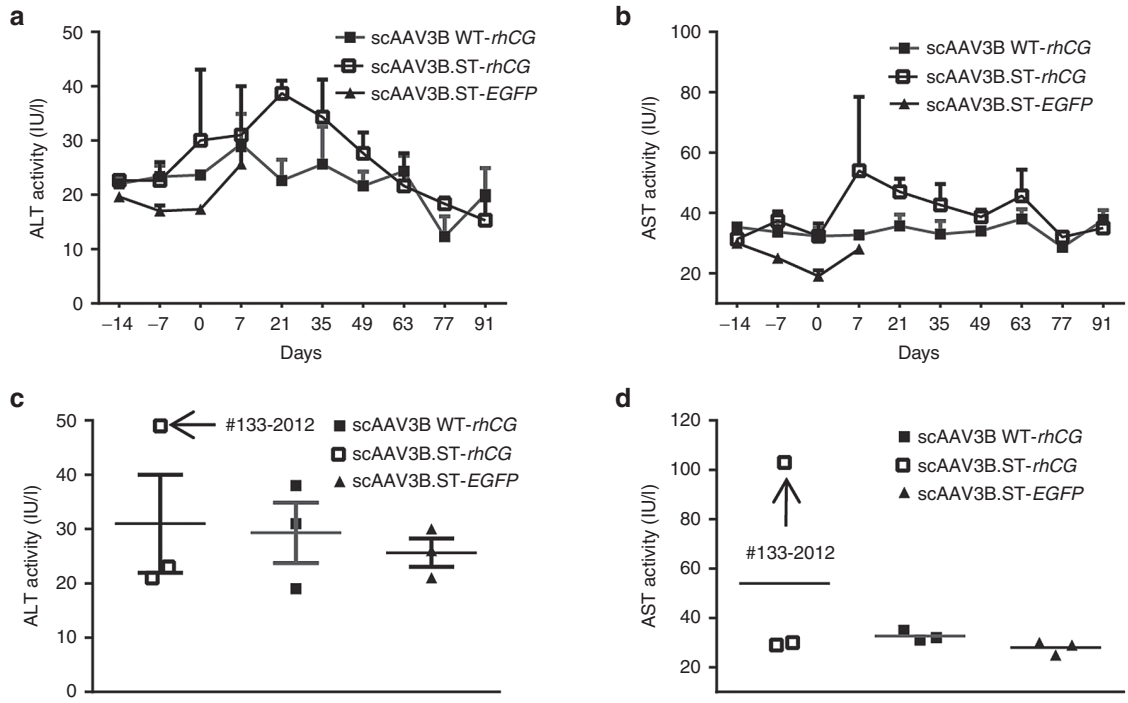

Figure 7 Lack apparent transaminitis in rhesus macaques by systemic delivery of WT and ST-modified rAAV3B vectors. Monkey sera were collected at different time points after vector infusion. The serum alanine aminotransferase (ALT) and aspartate aminotransferase (AST) levels were detected in New England Primate Research Center. The time courses of the ALT (**a**) and AST (**b**) levels as well as comparison of ALT (**c**) and AST (**d**) levels of different study groups at 7 days postinjection of vectors are presented. Analysis of variance was used for comparing the experimental results from the groups with WT rAAV3B and ST modified rAAV3B and they were determined to be statistically significant. $*P < 0.05$, $**P < 0.01$ versus WT rAAV3B-*rhCG*. No significant difference among all groups was observed.

for transducing human hepatocytes. This question proved to be particularly difficult to address since AAV8 failed to transduce any cell type, including hepatocytes *in vitro* (Figure 1).

In our quest to identify an alternative AAV serotype for efficient transduction of human hepatocytes, we made an unexpected observation nearly a decade ago that AAV3B vectors could transduce human liver cancer cells *in vitro* and human liver tumors in a xenograft mouse model *in vivo* remarkably well.[8,13,35] Although we also documented efficient transduction of primary human hepatocytes by AAV3B vector,[7] we did not directly compare its transduction efficiency with AAV2 or AAV8, which was performed in our current studies, to further corroborate the hepatotropic nature of AAV3B for human hepatocytes *in vitro*. However, since hepatocyte cultures *in vitro* do not truly represent their *in vivo* characteristics, we also attempted to evaluate the transduction efficiency of AAV3 vectors in a newly developed humanized murine model *in vivo*. In our studies, the transduction efficiency of AAV3 vector was comparable to AAV8. In this context, it is important to note that while our studies were in progress, Lisowski *et al.*[16] reported that a shuffled rAAV vector, designated LK03, which shares 97.7 and 98.9% homology with rAAV3B at the DNA and amino acids level, respectively, transduced human primary hepatocytes in a different humanized mouse model *in vivo*, but it was ~20-fold more efficient than AAV8. In our other studies with a different humanized liver xenograft mouse model,[36] we observed that AAV3B is ~12-fold more efficient than AAV8 in transducing human hepatocytes *in vivo*.[14] One of the caveats of using humanized murine models beyond serving as surrogates for initial human tropism screening is that they are generally immune-deficient in nature and thus do not account for the effect of humoral and cell mediated responses on transduction profile. In addition, such models are also limited by the absence of other human cells, tissues, organs, and components that invariably influence the ultimate transduction efficiency of AAV vectors in general. The transduction efficiency of AAV vectors in such xenograft murine models is also affected by possible donor-to-donor variations of human hepatocytes, as was reported recently.[37]

Our study also revealed a remarkable difference between AAV3B and AAV8 vectors in their capabilities to transduce murine liver (Figure 3). We have previously reported that AAV3B transduces human liver cells efficiently (confirmed by an average 27.7 ± 3.7% transduction of the engrafted human liver in our current study), because it utilizes human hepatocyte growth factor receptor (huHGFR) as a coreceptor,[8] and that even though murine HGFR (muHGFR) shares 88% identity with huHGFR,[38] AAV3B fails to bind to muHGFR because of the location of amino acid differences along the interaction interface, including amino residues that make contact with hepatocyte growth factor (HGF).[8] This could be a possible cause for poor transduction of murine liver (ranging from 1.4 ± 0.3 to 2.5 ± 2.3%) by AAV3B vector (Figure 3). AAV8, on the other hand, has previously been shown to utilize laminin receptor (LamR),[39] and it is possible that similar expression levels of LamR on murine and human liver cells account for the similar transductions of human (50.3 ± 7.0%) and murine (ranging from 33.5 ± 5.2 to 47.1 ± 4.7%) livers by AAV8 vector (Figure 3).

Given the limitations of hepatocyte cultures *in vitro*, and humanized mouse models *in vivo* outlined above, we next evaluated the safety and efficacy of AAV3B vectors in a NHP model *in vivo.* These studies were also prompted by the fact that, whereas huHGFR, a coreceptor for AAV3B,[8] shares only 88% identity with murine HGFR,[38] human and NHP HGFRs are 99% identical.[40] Our findings revealed the efficient liver-targeted gene transfer by WT AAV3B and optimized AAV3B.ST vectors following systematic administration. Remarkably, the vector-mediated EGFP expression and vector genome accumulation were largely restricted to the NHP liver. Although additional studies are warranted, based on our previously published data on AAV-mediated liver EGFP expression in other NHPs under the same exposure conditions (data not shown), we were able to conclude, with rough approximation, that scAAV3B vectors mediate comparable GFP expression in rhesus macaques as compared with scAAV9 in marmoset at a sixfold lower dose since 36% of hepatocytes on average were transduced by scAAV3B vectors 7 days postinjection, and as compared with 4–25% achieved by ssAAV7 in NHP liver following intraportal delivery at a threefold lower dose.[22,24]

Although the use of the EGFP reporter gene allowed us to address both vector tropism and gene transfer efficiency simultaneously, it was less quantitative and likely immunogenic leading to transient expression.[41] The use of a secreted self-antigen, rhCG, allowed us to study not only the efficiency, but also the onset and kinetics of transgene expression and long-term stability. In addition, since the rhCG used in this study can limit the potential host humoral and cellular immune responses to the transgene product, we were also able to evaluate the potential host immune responses against the vector capsid proteins for up to 3 months. The vector genome biodistribution study clearly revealed that the persisting vector genomes of AAV3B vectors were predominantly harbored in the monkey liver. Furthermore, the rhCG mRNA expression pattern in six selected organs displayed that the transgene expression was largely restricted to the liver, which also did not lead to any overt cytotoxicity. In addition, no obvious vector-related pathological changes in the liver, spleen and other organs were observed in any of the treated animals. Our studies are the first to document the remarkable specificity, efficacy, and safety of rAAV3B vectors in NHP livers following systemic administration. However, at least two frequent challenges encountered in performing such studies, which include the animal-to-animal variation due to their outbred nature, and the availability of only a limited number of animals largely due to the associated costs, warrant further investigations.

One of the major obstacles that limit the transduction efficiency of AAV vectors in general is ubiquitination, followed by proteasomal-mediated degradation,[42] which is triggered by phosphorylation of specific surface-exposed tyrosine (Y),[9,10] serine (S),[11] and/or threonine (T)[12] residues. Although we identified a specific combination of mutations (S663V+T492V) in the AAV3B capsid that significantly augmented the transduction efficiency of these vectors in liver cancer cells in a xenograft mouse model *in vivo*[15] in primary human hepatocytes *in vitro*; and in humanized mouse and NHP models *in vivo*, it should be noted that this most efficient mutant was identified from among 10 different permutations and combinations using a single human cancer cell line, Huh7, *in vitro*. Thus, it remains possible that one or more of the mutant AAV3B vectors will be optimal in transducing primary human hepatocytes in humanized mouse and NHP models *in vivo*. Although the ultimate value of one or more of these capsid-modified vectors will only be revealed by phase 1 clinical trials in humans, there is ample reason for the optimism that AAV3B vectors will prove to be a safer and more efficient alternative to AAV8 vectors for their potential use in gene therapy of human liver diseases.

MATERIALS AND METHODS

Production of recombinant AAV vectors. Preparation and purification of recombinant scAAV3B WT and ST mutant vectors expressing *EGFP* report gene and secreted β chain of rhesus chorionic gonadotropin (*rhCG*) gene have been described previously.[43] The transgenes were driven by a chicken β-action (CB) promoter in these constructs. All vector preparations used for the NHP studies were subjected to quality control tests including high-resolution transmission electron microscopy (EM), qPCR, and silver-stained sodium dodecyl sulfate–polyacrylamide gel electrophoresis as previously described.[44] The transgene expression was detected in Huh7.5 cells *in vitro*. All the AAV vectors were produced by the Viral Vector Core at University of Massachusetts Medical School Horae Gene Therapy Center (Worcester, MA).

AAV* in vitro *NAb assay, total IgG detection, and IgG subtyping assays. Rhesus macaque serum samples were heat inactivated at 56 °C for 30 minutes. *In vitro* NAb assays were performed on Huh7.5 cells as previously described,[45] and the limit of detection is 1:5 serum dilution. The normal mouse serum (Sigma-Aldrich, St. Louis, MO) was used as negative control. The AAV3B rabbit anti-serum and AAV3B-CMV-*LacZ* vectors were made by the Viral Vector Core at University of Massachusetts Medical School Horae Gene Therapy Center (Worcester, MA). The LacZ expression detection kit (Galacto-Star β-Galactosidase Reporter Gene Assay System for Mammalian Cells) was purchased from Life technologies (Carlsbad, CA).

AAV3B-specific IgG titers were determined by enzyme-linked immunosorbent assay (ELISA) as previously described.[46] Briefly, the AAV3B or AAV3B.ST vector particles were diluted in coating buffer (KPL, Gaithersburg, MD) to a final concentration of 2×10^{10} vector particles/ml. One hundred microliters of each were added to 96-well Nunc Maxisorp Immunoplate (Fisher Scientific, Newark, DE) for incubation at 4 °C overnight. Then, the plates were washed with wash buffer (0.05% Tween-20 in phosphate-buffered saline (PBS)), followed by blocking with blocking buffer (KPL, Gaithersburg, MD) for 2 hours at room temperature (RT). After wash, serum samples were diluted twofold serially in duplicate with a starting dilution of 1:400 and added to the plates for 1 hour incubation at RT. The biotin-conjugated goat anti-monkey IgG (Rockland Immunochemicals, Gilbertsville, PA) or biotin-conjugated goat anti-human IgG1, IgG2, IgG4 (Sigma-Aldrich, St Louis, MO) were diluted 20,000-folds in blocking buffer and added to the plates. After incubation for 1 hour at RT, the plates were washed four times. The avidin-Horseradish peroxidase (eBioscience, San Diego, CA) was added to plates and incubated for 1 hour at RT. Finally, plates were washed four times with wash buffer and developed with TMB in the dark for 15 minutes. The reaction was stopped with 2N H_2SO_4 and the OD at 450 nm was measured in a plate reader (BioTek, Winooski, VT).

Animal studies. All animal studies were performed in New England Primate Research Center at Harvard University (Southborough, MA) and under Institutional Animal Care and Use Committee (IACUC) approval by Harvard University. Male rhesus macaques (*Macaca mulatta*) at age of 1–2 years old were screened and selected for the animals without detectable NAb against AAV3B, purchased, treated and cared from New England Primate Research Center. Different vector dosing formulations were injected into rhesus macaques intravascularly via cephalic vein infusion. Monkey sera

were collected at different time points for detection of chemistry parameters including ALT and AST levels, which was performed by New England Primate Research Center. The serum rhCG expression was measured as described as following section. The tissues were collected at termination for detection of EGFP expression and pathological examination.

Humanized animals. FVB.Cg-Tg(SERPINA1*E342K)#Slcw mice[47] carrying the PiZ allele of the serpin peptidase inhibitor, clade A (α-1 antiproteinase, antitrypsin), member 1 (*Homo sapiens*) transgene were kindly provided by Dr. David Perlmutter, University of Pittsburgh School of Medicine. The PiZ allele of the SERPINA1* transgene was backcrossed five generations by a marker assisted speed congenic approach to the NOD.Cg-*Prkdc*^{scid}*Il2rg*^{tm1wjl}/SzJ (NSG) strain background. NSG-Tg(SERPINA1*E342K)#Slcw/Sz, abbreviated as NSG-PiZ mice, were intercrossed to fix the PiZ allele to homozygosity. Nine-week-old NSG-PiZ male mice were subjected to partial hepatectomy (2/3), then one million primary human hepatocytes (BioreclamationIVT, Westbury, NY; Product number: M00995) were injected to the mice via spleen. The mice sera were collected biweekly to determine the human albumin level using the ELISA kit (Bethyl Labs, Montgomery, TX; catalog no.: E80-129). All animal procedures were performed according to the guidelines of the IACUC of the University of Massachusetts Medical School.

In vivo *bioluminescence imaging and immunohistochemistry.* Eight weeks after human hepatocytes grafting, NSG-PiZ mice were intravenously injected with AAV vectors. Two weeks after vector delivery, all animals were intraperitoneally injected with 250 µl D-luciferin at a concentration of 15 mg/ml as previously described.[48] The luciferase activity was analyzed using *in vivo* imaging system (Xenogen IVIS 100). The total FFluc values were calculated using Living Image (PerkinElmer, Waltham, MA) and normalized with background subtraction of the same animal. For immunohistochemistry, mouse livers were harvested 4 weeks after AAV administration and frozen in optimal cutting temperature embedding medium. The frozen liver sections (8 µm) were fixed and permeablized in cold acetone, blocked with 13% (v/v) donkey serum (Sigma-Aldrich) and 8.7% (v/v) fetal bovine serum in PBS. For detection of human albumin-positive human hepatocypes, the primary goat polyclonal anti-human albumin antibody (1/200 dilution; Bethyl Labs; catalogue no. A80-129A) and the preadsorbed Alexa Fluor-568 donkey anti-goat IgG secondary antibody (1/1,000 dilution; Life Technologies, Carlsbad, CA; A-11057) were used. For detection of FFLuc, the mouse monoclonal anti-luciferase IgG1 (1/100 dilution; Invitrogen, Waltham, MA; Catalog No. 35–6700), the Horseradish peroxidase-conjugated goat anti-mouse IgG1 secondary antibody (1/2,000 dilution; Santa Cruz, Dallas, TX; Catalog No. sc-2060) and FITC-conjugated tyramide (PerkinElmer; FP1168) in Plus Amplification Diluent (PerkinElmer; FP1134) were applied. After staining, five images (20× objectives) from each xenograft liver section were analyzed using Leica DM-5500 microscope. The percentages of colocalization of human albumin and FFLuc signals on xenograft liver sections were estimated by ImarisColoc (Imaris, Bitplane, Belfast, UK).

***Detection of AAV-mediated EGFP transgene expression in liver* in vivo.** Fixed optimal cutting temperature-embedded liver sections from four hepatic lobes (left, middle, right and caudate) collected from the AAV3B.ST-EGFP vector-injected monkeys 7 days post injection were mounted on slides. As described in a previous publication,[1] the EGFP transduction efficiency was measured directly by GFP imaging in fixed sections using a Leica DM 5500B fluorescence microscope made by Leica microsystems (Buffalo Grove, IL). Images from one visual field per liver lobe were analyzed quantitatively using ImageJ analysis software (National Institutes of Health, Bethesda, MD). Transgene expression was assessed as total area of green fluorescence (GFP) (pixel2) per visual field (mean ± SEM). The GFP area fraction was calculated by ImageJ.

rhCG expression assay. An ELISA-based assay was used to detect serum rhCG level as described previously.[22] 518B7 anti-bovine LH coating antibody, primary Rabbit anti-rhCG antibody (Penn #5411), and Horseradish peroxidase-conjugated goat anti-rabbit IgG were obtained from University of Pennsylvania. rhCG standard was generated by transfecting rhCG expression plasmids into Huh7.5 cells and collecting the supernatant. Undiluted supernatant was arbitrarily assigned a concentration of 6,400 rU/ml (where rU = relative units). Other reagents for ELISA assay were purchased from KPL (Gaithersburg, MD). The samples were measured for OD at 450 nm in a luminometer (BioTek Instruments, Winooski, VT). The OD was used for data analyses, which are based on a linear regression comparison and interpolation of unknown samples against standard dilutions.

Detection of rhCG mRNA expression by RT-qPCR. The mRNA was isolated from the liver tissues collected from rhesus macaques at day 91 postinjection of WT- and ST-modified rAAV3B-*rhCG* vectors using Trizol (Life Technologies). Reverse transcription (RT) Taqman real-time qPCR was performed by the ViiA 7 real time PCR system (Life Technologies) to detect the rhCG mRNA expression level. All reagents, primers and probes were purchased from Life Technologies.

Vector biodistribution analysis. The tissue DNA samples were isolated using a Qiagen DNEasy kit (Qiagen, Valencia, CA). Detection and quantification of vector genomes in extracted DNA were performed by real-time qPCR as described previously.[1]

Toxicology studies. The first set of monkeys treated with AAV3B.ST-*EGFP* vectors was sacrificed 4 weeks postinjections, and the second set of animals treated with WT- and ST-modified scAAV3B-*rhCG* vectors was sacrificed 91 days postinjections. Each monkey was given an external and an internal gross examination. Tissues and organs were collected from each set and placed in 10% buffered formalin for fixation and processed for microscopic examination after Hematoxylin and Eosin staining in the pathology core at UMass Medical School.

Statistical analysis. Student *t*-test or analysis of variance was used to compare the test results among the different groups, and they were determined to be statistically significant when $P < 0.05$.

SUPPLEMENTARY MATERIAL

Table S1. Summary of the experimental design for the vector injection into animals.

Table S2. The prevalence of pre-existing NAbs against AAV3B in rhesus macaques.

Table S3. The titers of AAV3B-specific total IgG and its subtypes

Table S4. The summary of the blood chemical data of the rhesus macaques after vector delivery.

Figure S1. No EGFP transduction in the major organs other than liver by scAAV3B.ST-*EGFP* vector in rhesus macaques.

Figure S2. Histopathological analyses of liver and spleen from rhesus macaques administrated by WT or ST-modified rAAV3B vectors systematically.

ACKNOWLEDGMENTS

This research was supported by Public Health Service grant R21-NIBIB 1R21EB015684 (to A.S. and G.G.) a NIDDK R01-DK098252R01 (to T.R.F and C.M), an Office of the Director grant R24-OD018259 (to D.L.G, C.M, L.D.S., and M.A.B) from the National Institute Health and in part by a University of Massachusetts Medical School internal grant (to G.G.). G.G. is a founder of Voyager Therapeutics and holds equity in the company. G.G. is an inventor on patents with potential royalties licensed to Voyager Therapeutics and other biopharmaceutics.

REFERENCES

1. Ahmed, SS, Li, J, Godwin, J, Gao, G and Zhong, L (2013). Gene transfer in the liver using recombinant adeno-associated virus. *Curr Protoc Microbiol* **Chapter 14**: Unit14D.6.
2. Manno, CS, Pierce, GF, Arruda, VR, Glader, B, Ragni, M, Rasko, JJ *et al.* (2006). Successful transduction of liver in hemophilia by AAV-Factor IX and limitations imposed by the host immune response. *Nat Med* **12**: 342–347.

3. Nathwani, AC, Tuddenham, EG, Rangarajan, S, Rosales, C, McIntosh, J, Linch, DC *et al.* (2011). Adenovirus-associated virus vector-mediated gene transfer in hemophilia B. *N Engl J Med* **365**: 2357–2365.
4. Monteilhet, V, Saheb, S, Boutin, S, Leborgne, C, Veron, P, Montus, MF *et al.* (2011). A 10 patient case report on the impact of plasmapheresis upon neutralizing factors against adeno-associated virus (AAV) types 1, 2, 6, and 8. *Mol Ther* **19**: 2084–2091.
5. Li, C, Narkbunnam, N, Samulski, RJ, Asokan, A, Hu, G, Jacobson, LJ *et al.*; Joint Outcome Study Investigators. (2012). Neutralizing antibodies against adeno-associated virus examined prospectively in pediatric patients with hemophilia. *Gene Ther* **19**: 288–294.
6. Mingozzi, F, Maus, MV, Hui, DJ, Sabatino, DE, Murphy, SL, Rasko, JE *et al.* (2007). CD8(+) T-cell responses to adeno-associated virus capsid in humans. *Nat Med* **13**: 419–422.
7. Glushakova, LG, Lisankie, MJ, Eruslanov, EB, Ojano-Dirain, C, Zolotukhin, I, Liu, C *et al.* (2009). AAV3-mediated transfer and expression of the pyruvate dehydrogenase E1 alpha subunit gene causes metabolic remodeling and apoptosis of human liver cancer cells. *Mol Genet Metab* **98**: 289–299.
8. Ling, C, Lu, Y, Kalsi, JK, Jayandharan, GR, Li, B, Ma, W *et al.* (2010). Human hepatocyte growth factor receptor is a cellular coreceptor for adeno-associated virus serotype 3. *Hum Gene Ther* **21**: 1741–1747.
9. Zhong, L, Li, B, Mah, CS, Govindasamy, L, Agbandje-McKenna, M, Cooper, M *et al.* (2008). Next generation of adeno-associated virus 2 vectors: point mutations in tyrosines lead to high-efficiency transduction at lower doses. *Proc Natl Acad Sci USA* **105**: 7827–7832.
10. Markusic, DM, Herzog, RW, Aslanidi, GV, Hoffman, BE, Li, B, Li, M *et al.* (2010). High-efficiency transduction and correction of murine hemophilia B using AAV2 vectors devoid of multiple surface-exposed tyrosines. *Mol Ther* **18**: 2048–2056.
11. Aslanidi, GV, Rivers, AE, Ortiz, L, Govindasamy, L, Ling, C, Jayandharan, GR *et al.* (2012). High-efficiency transduction of human monocyte-derived dendritic cells by capsid-modified recombinant AAV2 vectors. *Vaccine* **30**: 3908–3917.
12. Aslanidi, GV, Rivers, AE, Ortiz, L, Song, L, Ling, C, Govindasamy, L *et al.* (2013). Optimization of the capsid of recombinant adeno-associated virus 2 (AAV2) vectors: the final threshold? *PLoS One* **8**: e59142.
13. Cheng, B, Ling, C, Dai, Y, Lu, Y, Glushakova, LG, Gee, SW *et al.* (2012). Development of optimized AAV3 serotype vectors: mechanism of high-efficiency transduction of human liver cancer cells. *Gene Ther* **19**: 375–384.
14. Ling, C, Wang, Y, Zhang, Y, Vercauteren, K, Verhoye, L, Lu, Y *et al.* (2014). Transduction of primary human hepatocytes in vitro and in humanized murine livers in vivo by recombinant AAV3 vectors. *Mol Ther* **22**: S2.
15. Ling, C, Wang, Y, Zhang, Y, Ejjigani, A, Yin, Z, Lu, Y *et al.* (2014). Selective *in vivo* targeting of human liver tumors by optimized AAV3 vectors in a murine xenograft model. *Hum Gene Ther* **25**: 1023–1034.
16. Lisowski, L, Dane, AP, Chu, K, Zhang, Y, Cunningham, SC, Wilson, EM *et al.* (2014). Selection and evaluation of clinically relevant AAV variants in a xenograft liver model. *Nature* **506**: 382–386.
17. Blacklow, NR, Hoggan, MD, Sereno, MS, Brandt, CD, Kim, HW, Parrott, RH *et al.* (1971). A seroepidemiologic study of adenovirus-associated virus infection in infants and children. *Am J Epidemiol* **94**: 359–366.
18. van der Marel, S, Comijn, EM, Verspaget, HW, van Deventer, S, van den Brink, GR, Petry, H *et al.* (2011). Neutralizing antibodies against adeno-associated viruses in inflammatory bowel disease patients: implications for gene therapy. *Inflamm Bowel Dis* **17**: 2436–2442.
19. Ling, C, Wang, Y, Feng, YL, Zhang, YN, Li, J, Hu, XR *et al.* (2015). Prevalence of neutralizing antibodies against liver-tropic adeno-associated virus serotype vectors in 100 healthy Chinese and its potential relation to body constitutions. *J Integr Med* **13**: 341–346.
20. Sprecher-Goldberger, S, Thiry, L, Lefébvre, N, Dekegel, D and de Halleux, F (1971). Complement-fixation antibodies to adenovirus-associated viruses, cytomegaloviruses and herpes simplex viruses in patients with tumors and in control individuals. *Am J Epidemiol* **94**: 351–358.
21. Zincarelli, C, Soltys, S, Rengo, G and Rabinowitz, JE (2008). Analysis of AAV serotypes 1-9 mediated gene expression and tropism in mice after systemic injection. *Mol Ther* **16**: 1073–1080.
22. Gao, G, Lu, Y, Calcedo, R, Grant, RL, Bell, P, Wang, L *et al.* (2006). Biology of AAV serotype vectors in liver-directed gene transfer to nonhuman primates. *Mol Ther* **13**: 77–87.
23. Gao, GP, Lu, Y, Sun, X, Johnston, J, Calcedo, R, Grant, R *et al.* (2006). High-level transgene expression in nonhuman primate liver with novel adeno-associated virus serotypes containing self-complementary genomes. *J Virol* **80**: 6192–6194.
24. Gao, G, Wang, Q, Calcedo, R, Mays, L, Bell, P, Wang, L *et al.* (2009). Adeno-associated virus-mediated gene transfer to nonhuman primate liver can elicit destructive transgene-specific T cell responses. *Hum Gene Ther* **20**: 930–942.
25. Gao, G, Bish, LT, Sleeper, MM, Mu, X, Sun, L, Lou, Y *et al.* (2011). Transendocardial delivery of AAV6 results in highly efficient and global cardiac gene transfer in rhesus macaques. *Hum Gene Ther* **22**: 979–984.
26. Dong, X, Tian, W, Wang, G, Dong, Z, Shen, W, Zheng, G *et al.* (2010). Establishment of an AAV reverse infection-based array. *PLoS One* 5: e13479.
27. Ellis, BL, Hirsch, ML, Barker, JC, Connelly, JP, Steininger, RJ, Porteus, MH (2013). A survey of *ex vivo*/*in vitro* transduction efficiency of mammalian primary cells and cell lines with nine natural adeno-associated virus (AAV1-9) and one engineered adeno-associated virus serotype. *Virol J* **10**: 74.
28. Wang, L, Calcedo, R, Wang, H, Bell, P, Grant, R, Vandenberghe, LH *et al.* (2010). The pleiotropic effects of natural AAV infections on liver-directed gene transfer in macaques. *Mol Ther* **18**: 126–134.
29. Wang, L, Calcedo, R, Bell, P, Lin, J, Grant, RL, Siegel, DL *et al.* (2011). Impact of pre-existing immunity on gene transfer to nonhuman primate liver with adeno-associated virus 8 vectors. *Hum Gene Ther* **22**: 1389–1401.
30. Gray, SJ, Matagne, V, Bachaboina, L, Yadav, S, Ojeda, SR and Samulski, RJ (2011). Preclinical differences of intravascular AAV9 delivery to neurons and glia: a comparative study of adult mice and nonhuman primates. *Mol Ther* **19**: 1058–1069.
31. Ponnazhagan, S, Mukherjee, P, Yoder, MC, Wang, XS, Zhou, SZ, Kaplan, J *et al.* (1997). Adeno-associated virus 2-mediated gene transfer in vivo: organ-tropism and expression of transduced sequences in mice. *Gene* **190**: 203–210.
32. Snyder, RO, Miao, CH, Patijn, GA, Spratt, SK, Danos, O, Nagy, D *et al.* (1997). Persistent and therapeutic concentrations of human factor IX in mice after hepatic gene transfer of recombinant AAV vectors. *Nat Genet* **16**: 270–276.
33. Mount, JD, Herzog, RW, Tillson, DM, Goodman, SA, Robinson, N, McCleland, ML *et al.* (2002). Sustained phenotypic correction of hemophilia B dogs with a factor IX null mutation by liver-directed gene therapy. *Blood* **99**: 2670–2676.
34. Nathwani, AC, Reiss, UM, Tuddenham, EG, Rosales, C, Chowdary, P, McIntosh, J *et al.* (2014). Long-term safety and efficacy of factor IX gene therapy in hemophilia B. *N Engl J Med* **371**: 1994–2004.
35. Ling, C, Lu, Y, Cheng, B, McGoogan, KE, Gee, SW, Ma, W *et al.* (2011). High-efficiency transduction of liver cancer cells by recombinant adeno-associated virus serotype 3 vectors. *J Vis Exp* **49**: Pii: 2538.
36. Vercauteren, K, Van Den Eede, N, Mesalam, AA, Belouzard, S, Catanese, MT, Bankwitz, D *et al.* (2014). Successful anti-scavenger receptor class B type I (SR-BI) monoclonal antibody therapy in humanized mice after challenge with HCV variants with *in vitro* resistance to SR-BI-targeting agents. *Hepatology* **60**: 1508–1518.
37. Bissig-Choisat, B, Wang, L, Legras, X, Saha, PK, Chen, L, Bell, P *et al.* (2015). Development and rescue of human familial hypercholesterolaemia in a xenograft mouse model. *Nat Commun* **6**: 7339.
38. Iyer, A, Kmiecik, TE, Park, M, Daar, I, Blair, D, Dunn, KJ *et al.* (1990). Structure, tissue-specific expression, and transforming activity of the mouse met protooncogene. *Cell Growth Differ* **1**: 87–95.
39. Akache, B, Grimm, D, Pandey, K, Yant, SR, Xu, H and Kay, MA (2006). The 37/67-kilodalton laminin receptor is a receptor for adeno-associated virus serotypes 8, 2, 3, and 9. *J Virol* **80**: 9831–9836.
40. Yan, G, Zhang, G, Fang, X, Zhang, Y, Li, C, Ling, F *et al.* (2011). Genome sequencing and comparison of two nonhuman primate animal models, the cynomolgus and Chinese rhesus macaques. *Nat Biotechnol* **29**: 1019–1023.
41. Velazquez, VM, Bowen, DG and Walker, CM (2009). Silencing of T lymphocytes by antigen-driven programmed death in recombinant adeno-associated virus vector-mediated gene therapy. *Blood* **113**: 538–545.
42. Duan, D, Yue, Y, Yan, Z, Yang, J and Engelhardt, JF (2000). Endosomal processing limits gene transfer to polarized airway epithelia by adeno-associated virus. *J Clin Invest* **105**: 1573–1587.
43. Ayuso, E, Mingozzi, F, Montane, J, Leon, X, Anguela, XM, Haurigot, V *et al.* (2010). High AAV vector purity results in serotype- and tissue-independent enhancement of transduction efficiency. *Gene Ther* **17**: 503–510.
44. Gao, G, and Sena-Esteves, M. Introducing genes into mammalian cells: viral vectors. In: Green, MR and J, Sambrook (eds). *Molecular Cloning*, vol. 3. Cold Spring Harbor Laboratory Press, Cold Spring Harbor, New York, 2012. pp. 1209–1334.
45. Calcedo, R, Vandenberghe, LH, Gao, G, Lin, J and Wilson, JM (2009). Worldwide epidemiology of neutralizing antibodies to adeno-associated viruses. *J Infect Dis* **199**: 381–390.
46. Hurlbut, GD, Ziegler, RJ, Nietupski, JB, Foley, JW, Woodworth, LA, Meyers, E *et al.* (2010). Preexisting immunity and low expression in primates highlight translational challenges for liver-directed AAV8-mediated gene therapy. *Mol Ther* **18**: 1983–1994.
47. Carlson, JA, Rogers, BB, Sifers, RN, Finegold, MJ, Clift, SM, DeMayo, FJ *et al.* (1989). Accumulation of PiZ alpha 1-antitrypsin causes liver damage in transgenic mice. *J Clin Invest* **83**: 1183–1190.
48. Wang, LN, Wang, Y, Lu, Y, Yin, ZF, Zhang, YH, Aslanidi, GV *et al.* (2014). Pristimerin enhances recombinant adeno-associated virus vector-mediated transgene expression in human cell lines *in vitro* and murine hepatocytes in vivo. *J Integr Med* **12**: 20–34.